Volume 9 | Number 28 | 28 July 2018 | Pages 6009–6158

Chemical Science

rsc.li/chemical-science

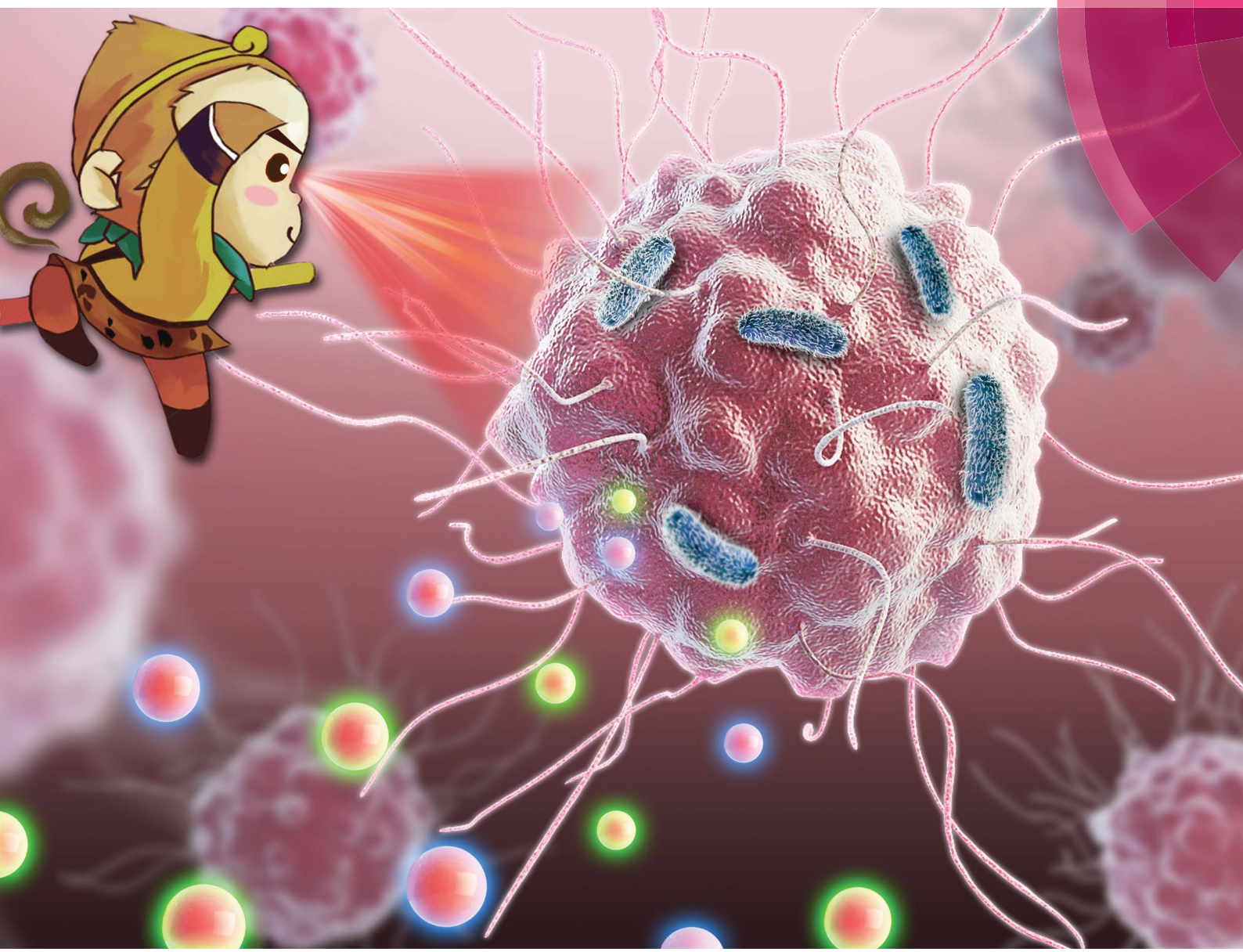

ISSN 2041-6539

ROYAL SOCIETY OF CHEMISTRY

EDGE ARTICLE

Chunya Li, Zhihong Liu *et al.*

Design of a ratiometric two-photon probe for imaging of hypochlorous acid (HClO) in wounded tissues

Chemical Science

EDGE ARTICLE

View Article Online
View Journal | View Issue

Cite this: *Chem. Sci.*, 2018, **9**, 6035

Design of a ratiometric two-photon probe for imaging of hypochlorous acid (HClO) in wounded tissues†

Zhiqiang Mao,‡[a] Miantai Ye,‡[a] Wei Hu,[b] Xiaoxue Ye,[a] Yanying Wang,[a] Huijuan Zhang,[a] Chunya Li *[a] and Zhihong Liu *[b]

HClO plays crucial roles in a wide range of biological and pathological processes. Recent studies have revealed that the generation of HClO has close links with the wound healing process. It's thus meaningful to develop a reliable method for monitoring HClO in wounded tissues. Toward this purpose, we herein report a rationally designed quinolone-based ratiometric two-photon fluorescent probe, **QClO**, for HClO. The probe **QClO** rapidly displays a drop in blue emission and an increase of green emission in response to HClO due to the oxidation of oxathiolane. The fluorescence intensity ratio (green/blue) can serve as the ratiometric detection signal for HClO with high sensitivity. After confirming its excellent sensing performance *in vitro*, the probe was validated by detecting exogenous and endogenous HClO in living cells. The probe was capable of monitoring HClO *in situ* in the wounded tissues of mice by two-photon microscopy, which demonstrated the production profile of HClO during the wound-healing process. This work affords a simple and reliable tool for the detection and imaging of HClO, which promises to find more applications in HClO-related biological and pathological studies.

Received 13th April 2018
Accepted 14th May 2018

DOI: 10.1039/c8sc01697f

rsc.li/chemical-science

Introduction

Reactive oxygen species (ROS) are endogenously generated signalling molecules, which play vital roles in a broad range of physiological and pathological processes.[1–3] Among the various ROS, hypochlorous acid (HClO) has triggered enormous interest in biological and medical science. Endogenous HClO is produced by the heme enzyme myeloperoxidase (MPO)-catalysed reaction between hydrogen peroxide and chloride ions.[4] HClO plays a critical role in the host resistance to microbial pathogens in the innate immune response; it is also known that excessive amounts of HClO can oxidize various biomolecules including nucleic acids, proteins, cholesterol and lipids, leading to cell and tissue damage.[5] Mounting evidence has established a firm correlation between HClO and various biological and pathological activities ranging from inflammatory diseases to cancer, and immune and neurological diseases.[6–8] For these reasons, it is imperative to develop reliable methods to evaluate the fluctuation of HClO levels in cells and tissues.

To date, fluorescence imaging has been considered as one of the versatile ways to detect and trace substances in living systems, owing to its unique advantages such as simplicity, high sensitivity and non-invasive visualization features. As such, a number of fluorescent probes have been designed for the detection and imaging of HClO.[9–18] Nonetheless, most of them are one-photon fluorescent probes, which are excited with short wavelengths such UV or visible light and, consequently, suffer from shallow imaging depth, considerably impeding their application in *in vivo* and *ex vivo* imaging. One promising approach to surmount the problem is to develop a two-photon fluorescent probe for two-photon microscopy (TPM). TPM utilizes two near-infrared photons to excite the fluorophore, leading to incomparable advantages in fluorescence imaging, such as deeper imaging depth, less photobleaching and background fluorescence, and higher temporal–spatial resolution than one-photon fluorescent probes.[19–24] Up to now, however, only a few two-photon fluorescent probes for HClO have been reported.[25–28] Among them, only one probe can afford a ratiometric signal for sensing.[28] As known, single fluorescence intensity-based probes are easily encountered with some substantial interferences, such as the variation of environment polarity, pH, photobleaching, probe concentration, probe distribution, laser power, *etc.* In contrast, ratiometric fluorescent probes with two emission bands can effectively mitigate the above-mentioned interferences owing to the built-in self-

[a]*Key Laboratory of Analytical Chemistry of the State Ethnic Affairs Commission, College of Chemistry and Materials Science, South-Central University for Nationalities, Wuhan 430074, China. E-mail: lichychem@163.com*

[b]*Key Laboratory of Analytical Chemistry for Biology and Medicine (Ministry of Education), College of Chemistry and Molecular Sciences, Wuhan University, Wuhan 430072, China. E-mail: zhhliu@whu.edu.cn*

† Electronic supplementary information (ESI) available. See DOI: 10.1039/c8sc01697f

‡ These authors contributed equally.

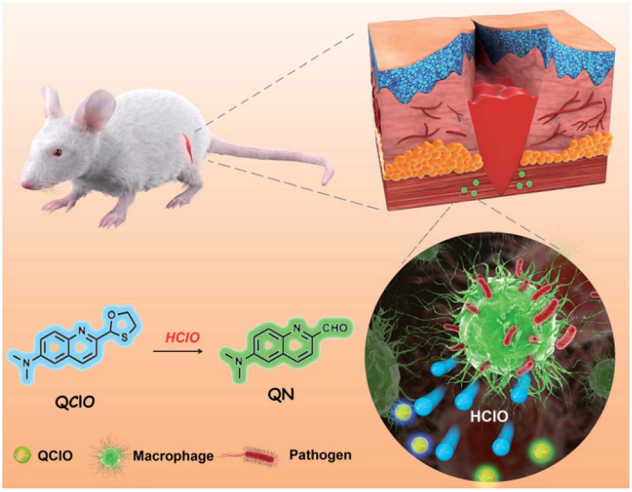

Scheme 1 Design of a TP fluorescent probe, **QClO**, for the ratiometric monitoring of HClO in wounded tissues of mice.

calibration function.[29–32] Apart from the signalling channel, there are also other concerns with the reported probes for HClO. For example, the only ratiometric probe[28] exhibits a rather large cross-talk between the two emissions ($\Delta\lambda_{em}$ = 35 nm), which may cause spectral overlap and decrease the sensing sensitivity.

Recent research results have revealed that ROS are of paramount importance in the wound healing processes of animals and human beings. Indeed, ROS as secondary messengers can recruit immunocytes and lymphoid cells to the wounded site, regulate the formation of blood vessels and kill invading pathogens.[33,34] Previous studies have validated the significant roles of H_2O_2, NO and $ONOO^-$ in the tissue repairing process by the fluorescence imaging method,[35–38] but the role of HClO in the wound healing process is still elusive due to the lack of reliable and convenient tools for imaging this molecule in tissues.

To meet the great demand, a ratiometric two-photon fluorescent probe, **QClO**, for HClO was proposed in this work. The probe itself displayed an emission peak at 492 nm. After its reaction with HClO, the probe was oxidized to 6-(dimethylamino) quinoline-2-carbaldehyde (**QN**) and a new emission band emerged at 562 nm. Thus, the probe presented ratiometric signals for highly sensitive detection of HClO. The two-photon excitation nature also endows the probe with good performance in detecting endogenous and exogenous HClO in living cells, as well as the ability to monitor subtle variations of HClO in wounded tissues of mice by two-photon microscopy (Scheme 1). To the best of our knowledge, **QClO** is the first ratiometric two-photon fluorescent probe for tracing the generation of HClO in the wound healing process in living tissues.

Results and discussion

Design and synthesis of QClO

Due to the low content and potent oxidation capacity of ROS, it's difficult to specifically detect HClO in the presence of other ROS in biological environments. Recently, the thioketal protecting acetyl group was reported to be easily oxidized by HClO to release the acetyl group, which can serve as a sensitive and selective recognition moiety for HClO.[26,39] With this in mind, we sought to use this unique reaction to design an intermolecular charge transfer (ICT) principle based ratiometric fluorescent probe. Developing a ratiometric probe requires that the probe itself and its reaction product are both highly fluorescent. Combined with these considerations, we rationally designed and synthesized a new ratiometric two-photon fluorescent probe, **QClO** (*N*,*N*-dimethyl-2-(1,3-oxathiolan-2-yl)quinolin-6-amine), for the detection and imaging of HClO (Scheme S1†). In the probe, a quinolone scaffold was chosen as a two-photon fluorophore due to its verified excellent two-photon absorption properties,[40–43] and its thioketal protected aldehyde as the HClO recognition moiety. After reaction with HClO, the oxathiolane group of **QClO** was deprotected to form a typical "push–pull" structure (6-(dimethylamino)quinoline-2-carbaldehyde). The "push–pull" structure is favourable for two-photon absorption properties and displays a red-shifted fluorescence emission owing to the enhanced "ICT" effect.[44–46] It was thus safe to envision that the probe would show ratiometric fluorescence emissions in response to HClO under two-photon excitation. The probe **QClO** was synthesized and characterized by ^{1}H NMR, ^{13}C NMR and HRMS (Fig. S12–S17†).

Spectral response of QClO to HClO

As the first step, the response performance of **QClO** toward HClO was investigated in 10 mM PBS buffer solution (pH = 7.4, containing 5% DMF) at room temperature. The probe itself displays a maximal absorption at 360 nm (ε = 2.2 × 10^4 M^{-1} cm^{-1}) and a fluorescence emission band centered at 492 nm (ε = 0.32) (Fig. S1†). Upon the addition of HClO, a new emission band centered at 562 nm emerged and concomitantly the emission peak at 492 nm was remarkably decreased owing to the oxidation of the thioketal protected aldehyde (Fig. 1a). Upon increasing the amount of HClO, the emission band of the probe was gradually shifted from the cyan region (492 nm) to the green region (562 nm), suggesting that the probe can be utilized for the ratiometric detection of HClO (Fig. 1b). The titration curve illustrated that the ratio of $I_{562\ nm}/I_{492\ nm}$ showed a linear response to the HClO concentration in the range from 0.8 to 12.5 μM (R^2 = 0.98) (Fig. 1c). And the limit of detection (LOD) value was calculated to be 89 nM according to $3S_b/m$ (where S_b is the standard deviation of the blank (n = 11) and m is the slope for the range of linearity), indicating that the probe has high sensitivity toward HClO. After reacting with 25 μM excess HClO, the probe exhibited a maximal ratio value of 4.0, which is significantly larger than those of previously reported HClO probes (Table S1†). Upon the addition of varied amounts (10, 16, and 24 μM) of HClO, the fluorescence ratio of $I_{562\ nm}/I_{492\ nm}$ rapidly reached the plateau in 60 s, which confirmed that the probe can react with HClO quickly, and that it holds great promise in the real-time detection of HClO *in vitro* and *in vivo* (Fig. 1d).

The selectivity of the probe toward HClO and other potential interfering species including metal ions (Ca^{2+}, Mg^{2+}, Zn^{2+}, Mn^{2+}, and Fe^{2+}), biothiols (Cys, Hcy, and GSH), ROS (H_2O_2, O_2^-, and $^{\bullet}OH$) and RNS ($ONOO^-$ and NO) was studied. As shown in

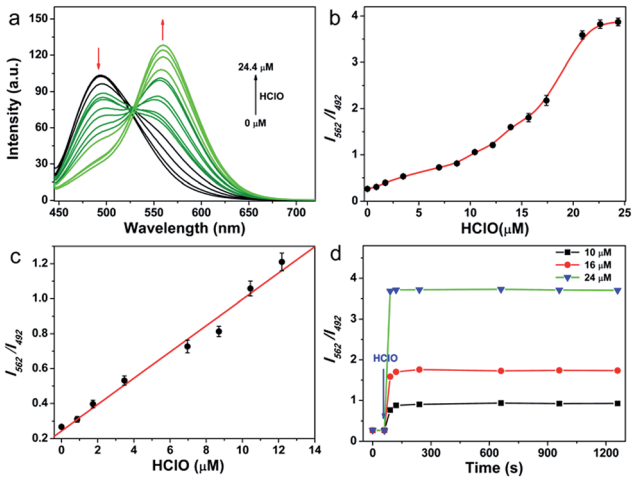

Fig. 1 (a) Fluorescence spectra of 5.0 μM **QClO** upon the addition of HClO (0–24.4 μM). (b) Plot of the fluorescence intensity ratio (562 nm/492 nm) change of 5.0 μM **QClO** *versus* ClO^- concentration (0–24.4 μM). (c) Linear relationship between the fluorescence intensity ratio and HClO concentration in the range of 0.8–12.5 μM. (d) Plot of the fluorescence intensity ratio of **QClO** as a function of HClO (10, 16, and 24 μM). The excitation wavelength was 426 nm in 10 mM PBS (pH = 7.4, containing 5% DMF) buffer solution.

Fig. S4,† none of the interfering species caused any fluorescence enhancement or ratio ($I_{562\ nm}/I_{492\ nm}$) change. Only HClO induced a significant fluorescence change. pH-sensitivity is another essential criterion to evaluate whether a probe can be applied in complex cellular environments. We then tested the pH effect on the response of the probe **QClO** to HClO. Delightfully, the probe showed signals unaffected by variations of pH in the pH range of 5.0–8.5 (Fig. S5†), while the fluorescence ratio was pH-independent in the pH range of 7.0–9.0 (Fig. S6†), strongly suggesting that the probe can work in the physiological pH range. Thus, it is reasonable to conclude that the probe shows a sensitive and selective response to HClO in a physiological pH range.

Reaction mechanism study

Subsequently, we identified the reaction product between the probe and HClO. The reaction mixture of **QClO** and excess HClO in PBS solution exhibited maximal absorption at 414 nm and emission at 562 nm, the same as the maximum absorption (414 nm) and emission (563 nm) of QN (Fig. S2 and S3†). Furthermore, we conducted EI-MS analysis of the reaction mixture of **QClO** and HClO. The MS spectra showed a significant *m*/*z* peak at 200.12, which evidently supported that the main product was the compound QN (200.09) (Fig. S7†). The optical properties and MS data reasonably rationalized the proposed sensing mechanism: the probe **QClO** was first oxidized to a sulfoxide compound and then oxidized to an unstable sulphone compound, which was subsequently hydrolyzed to yield the fluorescent compound QN (Scheme S2†).

Two-photon properties for QClO

In order to prove that the probe can be used in two-photon microscopy, the two-photon absorption properties of **QClO** and the reaction product of **QClO** and HClO were measured in 10 mM PBS buffer (pH = 7.4, containing 5% DMF) (Fig. S8†). The probe **QClO** showed a maximum two-photon action cross section ($\Phi\delta$) value of 25 GM at 810 nm, while the reaction product of **QClO** treated with HClO showed a maximal $\Phi\delta$ value of 37 GM at 820 nm. The two-photon absorption and emission properties of **QClO** in the absence/presence of HClO suggest that the probe is ideal for ratiometric detection and imaging of HClO under two-photon microscopy.

Two-photon imaging of HClO in living cells

Prior to applying the probe for the biological imaging, we assessed the cytotoxicity of **QClO** with HeLa cells by the MTT method (Fig. S9†). The results illustrated that the probe has a low cytotoxicity even with concentrations up to 20 μM (cell viability > 80%), which suggests the probe is safe for visualizing HClO in living cells. To confirm the capability of the probe in detecting HClO in living cells, HeLa cells were incubated with 5.0 μM probe **QClO**. As expected, the **QClO** loaded HeLa cells showed strong fluorescence in the blue channel (450–500 nm) and negligible fluorescence in the green channel (550–650 nm) under TPM (Fig. 2a–c). Upon the addition of 50 μM HClO for 30 min, a significant decrease of blue fluorescence and a remarkable enhancement of green fluorescence were observed (Fig. 2d–f). Furthermore, the fluorescence change of blue and green channels can be quantitatively compared from the fluorescence ratio (green/blue). Compared with the control, the addition of 50 μM HClO resulted in 2.3-fold enhancement of the fluorescence ratio (Fig. 2i). The results clearly confirmed that the probe can detect exogenous HClO change under two-photon microscopy.

Next, the potential utility of **QClO** as a probe for visualizing endogenous HClO in living cells was evaluated. It has been well documented that RAW 264.7 cells can produce HClO upon the stimulation of lipopolysaccharide (LPS) and phorbol-12-myristate-13-acetate (PMA).[47–49] The RAW 264.7 cells were initially incubated with 5.0 μM **QClO**, and the cells displayed

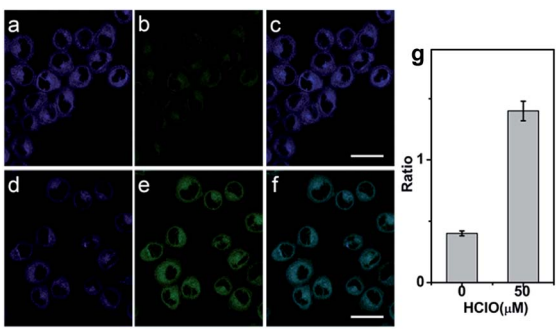

Fig. 2 TP images of exogenous HClO with **QClO** in HeLa cells. HeLa cells were treated with 5.0 μM **QClO** for 0.5 h (a, b, and c) and then with 50 μM HClO for 0.5 h (d, e, and f). (g) Fluorescence intensity ratios from overlay images of (c) and (f). The fluorescence intensities were collected at the blue channel (400–500 nm) and the green channel (550–600 nm) respectively upon two-photon excitation at 820 nm. Scale bar: 20 μm. Incubation time: 0.5 h.

bright blue fluorescence in the blue channel and faint green fluorescence in the green channel under TPM (Fig. 3a–c).

Interestingly, a drop in blue fluorescence and a sharp increase of green fluorescence were observed in the LPS and PMA pretreated **QClO**-loaded cells, which can be ascribed to the reaction of HClO and **QClO**. The cells pretreated with HClO stimulants showed 3.5-fold enhancement of the fluorescence ratio (green/blue) compared to that of the control (Fig. 3d–f). To further verify the change in the fluorescence ratio caused by HClO, the cells were initially treated with LPS, PMA and 4-aminobenzoic acid hydrazide (ABH, a well-known MPO inhibitor) and then incubated with **QClO**. The cells exhibited much weaker fluorescence in the green channel and the fluorescence ratio (green/blue) was close to the ratio of the control, which was the result of the inhibition of MPO activity, and induced decrease in the intracellular HClO production (Fig. 3g–j). All these results clearly demonstrated that the probe is promising and effective for detecting and imaging the subtle variations of exogenous and endogenous HClO levels under two-photon microscopy.

Two-photon imaging of HClO in mouse liver tissues

During the wound healing process, the wounded tissues can recruit macrophages and produce a high local concentration of ROS including HClO to defend them against the invading pathogens.[50,51] To the best of our knowledge, there is no report on the utilization of a two-photon fluorescent probe for HClO detection in wounded tissues, perhaps due to the limitations of current probes such as low sensitivity and slow reaction rate, inaccuracy of the single intensity signal readout, and limited imaging depth, which have not been overcome. With this aim in mind, we first applied the probe for tissue imaging by two-photon microscopy (Fig. S10†). The **QClO** stained mice liver tissues displayed bright blue fluorescence emission and faint green fluorescence emission. After the treatment with HClO, the **QClO**-stained tissues exhibited enhanced green fluorescence intensity and weak blue fluorescence intensity due to the reaction of **QClO** and HClO, which is similar to that in cells. The fluorescence change of blue and green channels can also be quantified by the fluorescence ratio (green/blue). To examine the imaging depth of TPM, the liver tissue fluorescence intensities at different depths were recorded using a two-photon microscope in the *z*-scan model. The *z*-stack images clearly revealed that the image depth was up to *ca.* 180 μm, which is indubitable evidence that **QClO** can track HClO in deep tissue under TPM (Fig. S11†).

Tracking HClO in wounded tissues of mice

Motivated by the deep imaging depth in tissues, we attempted to probe HClO in the wound of mice by two-photon microscopy. First, the mice were treated with or without a man-made wound on the left rear leg for different days (1 day and 4 days). Then,

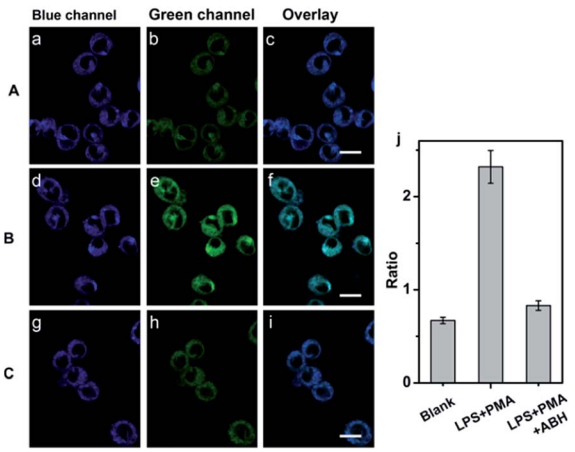

Fig. 3 TP images of endogenous HClO with **QClO** in RAW 264.7 cells. (a–c) RAW 264.7 cells were incubated with 5.0 μM **QClO** for 0.5 h. (d–f) RAW 264.7 cells pretreated with HClO stimulants (1.0 μg mL^{-1} LPS and 1.0 μg mL^{-1} PMA) for 6 h and then incubated with 5.0 μM **QClO** for 0.5 h. (g–i) RAW 264.7 cells pretreated with HClO stimulants (1.0 μg mL^{-1} LPS and 1.0 μg mL^{-1} PMA) and 200 μM ABH for 6 h and then incubated with 5.0 μM **QClO** for 0.5 h. (j) Fluorescence intensity ratios from overlay images of c, f and i. The fluorescence intensities were collected at the blue channel (400–500 nm) and green channel (550–600 nm) upon two-photon excitation at 820 nm. Scale bar: 10 μm.

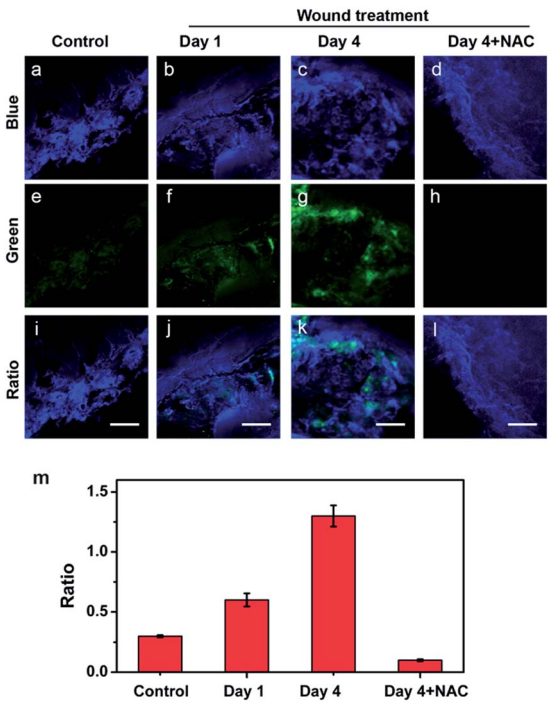

Fig. 4 TP images of the HClO level in wounded tissues of mice with **QClO**. The control mice and wounded mice were injected with 150 μL of 1.0 mM **QClO** for 1.0 h, respectively, and the tissues were harvested and imaged. (a, e, and i) TP images of the control mice tissues. (b, f, and j) TP images of the wounded tissues of mice at day 1. (c, g, and k) TP images of the wounded tissues of mice at day 4. (d, h, and l) The wounded mice at day 4 were injected with 150 μL of 1.0 mM **QClO** and 5.0 mM NAC for 1.0 h, and then the tissues were harvested and imaged. (m) Fluorescence ratios (green/blue) of the ratio images (i), (j), (k) and (l). The fluorescence emissions were collected at the blue channel (a–d, 400–500 nm) and green channel (e–h, 550–600 nm) upon excitation at 820 nm. Scale bar: 50 μm.

150 μL of 1.0 mM probe was administered underneath the wounded areas *via* subcutaneous injection. After the treatment, the wounded tissues were harvested and imaged under a two-photon microscope. As shown in Fig. 4a, e and i, the tissues of the control mice showed bright blue fluorescence and rather weak green fluorescence. The fluorescence changes of the two channels can also be evaluated by the fluorescence ratio (green/blue). In contrast, the wounded tissues (days 1 and 4) displayed much lower blue fluorescence and significantly brighter green fluorescence, indicating HClO was overproduced in the wound healing process (Fig. 4b, c, and f and 4c, g, and k). To further confirm that the changes of the fluorescence ratio were caused by HClO, a group of mice with the same wound at day 4 were subcutaneously injected with 150 μL of 1.0 mM probe and 5.0 mM NAC (HClO scavenger) in the wounded areas. As a result, the fourth group of mice treated with **QClO** and NAC synchronously displayed faint green fluorescence and strong blue fluorescence, together with a much lower fluorescence ratio close to that of the control (Fig. 4m). All the two-photon imaging results demonstrated that **QClO** can be used for probing and monitoring the fluctuation of the HClO level in the wound healing process from a living animal under TPM.

Conclusions

In summary, a quinolone-based two-photon fluorescent probe, **QClO**, for ratiometric detection and imaging of HClO in wounded tissues was rationally developed and characterized. The probe **QClO** showed a drop in blue emission and an increase of green emission in response to the presence of HClO in a short time (<1 min), which provided a ratiometric detection manner for HClO. The probe can realize ratiometric detection of HClO *in vitro* with a linear range of 0.8–12 μM and a limit of detection value of 89 nM. Furthermore, the probe can also visualize the fluctuation of exogenous and endogenous HClO levels in living cells, respectively, under two-photon microscopy. Owing to the excellent sensing performance and two-photon excitation nature, the probe successfully revealed the over-production of HClO in the wounded tissue area. To the best of our knowledge, **QClO** is the first two-photon fluorescent probe to monitor the generation of HClO during the wound healing process of mice. This work not only creates an effective ratiometric two-photon fluorescent probe for the selective and sensitive detection of HClO but also offers a technological platform for visualizing HClO in biological activities.

Conflicts of interest

There are no conflicts to declare.

Acknowledgements

The work was finally supported by the National Natural Science Foundation of China (Grant Nos 21675175 and 21625503), the Natural Science Foundation of Hubei Province, China (Grant Nos 2015CFA02) and the Major Projects of Technical Innovation of Hubei Province, China (No. 2017ACA172). We also thank the Optical Bioimaging Core Facility of WNLO-HUST for the support with two-photon microscopy. All animal studies were performed in accordance with the Guidelines for the Care and Use of Laboratory Animals of the Chinese Animal Welfare Committee and approved by the Institutional Animal Care and Use Committee, Wuhan University Center for Animal Experiment, Wuhan, China.

Notes and references

1 B. C. Dickinson and C. J. Chang, *Nat. Chem. Biol.*, 2011, **7**, 504–511.
2 S. S. Sabharwal and P. T. Schumacker, *Nat. Rev. Cancer*, 2014, **14**, 709–721.
3 D. Trachootham, J. Alexandre and P. Huang, *Nat. Rev. Drug Discovery*, 2009, **8**, 579–591.
4 S. J. Klebanoff, A. J. Kettle, H. Rosen, C. C. Winterbourn and W. M. Nauseef, *J. Leukocyte Biol.*, 2013, **93**, 185–198.
5 F. C. Fang, *Nat. Rev. Microbiol.*, 2004, **2**, 820–832.
6 D. I. Pattison and M. J. Davies, *Curr. Med. Chem.*, 2006, **13**, 3271–3290.
7 C. Gorrini, I. S. Harris and T. W. Mak, *Nat. Rev. Drug Discovery*, 2013, **12**, 931–947.
8 J. Yang, X. Zhang, P. Yuan, J. Yang, Y. Xu, J. Grutzendler, Y. Shao, A. Moore and C. Ran, *Proc. Natl. Acad. Sci. U. S. A.*, 2017, **114**, 12384–12389.
9 M. Sun, H. Yu, H. Zhu, F. Ma, S. Zhang, D. Huang and S. Wang, *Anal. Chem.*, 2014, **86**, 671–677.
10 H. Zhu, J. Fan, J. Wang, H. Mu and X. Peng, *J. Am. Chem. Soc.*, 2014, **136**, 12820–12823.
11 Q. A. Best, N. Sattenapally, D. J. Dyer, C. N. Scott and M. E. McCarroll, *J. Am. Chem. Soc.*, 2013, **135**, 13365–13370.
12 J. J. Hu, N.-K. Wong, M.-Y. Lu, X. Chen, S. Ye, A. Q. Zhao, P. Gao, R. Y.-T. Kao, J. Shen and D. Yang, *Chem. Sci.*, 2016, **7**, 2094–2099.
13 H. Ma, B. Song, Y. Wang, D. Cong, Y. Jiang and J. Yuan, *Chem. Sci.*, 2017, **8**, 150–159.
14 P. Wei, W. Yuan, F. Xue, W. Zhou, R. Li, D. Zhang and T. Yi, *Chem. Sci.*, 2018, **9**, 495–501.
15 B. Zhu, P. Li, W. Shu, X. Wang, C. Liu, Y. Wang, Z. Wang, Y. Wang and B. Tang, *Anal. Chem.*, 2016, **88**, 12532–12538.
16 Y. Tang, D. Lee, J. Wang, G. Li, J. Yu, W. Lin and J. Yoon, *Chem. Soc. Rev.*, 2015, **44**, 5003–5015.
17 S. Kenmoku, Y. Urano, H. Kojima and T. Nagano, *J. Am. Chem. Soc.*, 2007, **129**, 7313–7318.
18 J. Wu, Z. Li, L. Yang, J. Han and S. Han, *Chem. Sci.*, 2013, **4**, 460–467.
19 H. M. Kim and B. R. Cho, *Chem. Rev.*, 2015, **115**, 5014–5055.
20 L. Zhou, X. Zhang, Q. Wang, Y. Lv, G. Mao, A. Luo, Y. Wu, Y. Wu, J. Zhang and W. Tan, *J. Am. Chem. Soc.*, 2014, **136**, 9838–9841.
21 Z. Mao, H. Jiang, X. Song, W. Hu and Z. Liu, *Anal. Chem.*, 2017, **89**, 9620–9624.
22 H. W. Liu, Y. Liu, P. Wang and X. B. Zhang, *Methods Appl. Fluoresc.*, 2017, **5**, 012003.
23 J. Zhang, X. Y. Zhu, X. X. Hu, H. W. Liu, J. Li, L. L. Feng, X. Yin, X. B. Zhang and W. Tan, *Anal. Chem.*, 2016, **88**, 11892–11899.

24 H. W. Liu, X. B. Zhang, J. Zhang, Q. Q. Wang, X. X. Hu, P. Wang and W. Tan, *Anal. Chem.*, 2015, **87**, 8896–8903.
25 Q. Xu, C. H. Heo, G. Kim, H. W. Lee, H. M. Kim and J. Yoon, *Angew. Chem., Int. Ed.*, 2015, **54**, 4890–4894.
26 L. Yuan, L. Wang, B. K. Agrawalla, S. J. Park, H. Zhu, B. Sivaraman, J. Peng, Q. H. Xu and Y. T. Chang, *J. Am. Chem. Soc.*, 2015, **137**, 5930–5938.
27 Q. Xu, C. H. Heo, J. A. Kim, H. S. Lee, Y. Hu, D. Kim, K. M. Swamy, G. Kim, S. J. Nam, H. M. Kim and J. Yoon, *Anal. Chem.*, 2016, **88**, 6615–6620.
28 Y. W. Jun, S. Sarkar, S. Singha, Y. J. Reo, H. R. Kim, J. J. Kim, Y. T. Chang and K. H. Ahn, *Chem. Commun.*, 2017, **53**, 10800–10803.
29 K. Gu, Y. Xu, H. Li, Z. Guo, S. Zhu, S. Zhu, P. Shi, T. D. James, H. Tian and W. H. Zhu, *J. Am. Chem. Soc.*, 2016, **138**, 5334–5340.
30 T. F. Brewer, G. Burgos-Barragan, N. Wit, K. J. Patel and C. J. Chang, *Chem. Sci.*, 2017, **8**, 4073–4081.
31 Q. Wan, S. Chen, W. Shi, L. Li and H. Ma, *Angew. Chem., Int. Ed.*, 2014, **53**, 10916–10920.
32 M. H. Lee, J. S. Kim and J. L. Sessler, *Chem. Soc. Rev.*, 2015, **44**, 4185–4191.
33 A. Sindrilaru, T. Peters, S. Wieschalka, C. Baican, A. Baican, H. Peter, A. Hainzl, S. Schatz, Y. Qi, A. Schlecht, J. M. Weiss, M. Wlaschek, C. Sunderkötter and K. J. Scharffetter-Kochanek, *J. Clin. Invest.*, 2011, **121**, 985–997.
34 C. Dunnill, T. Patton, J. Brennan, J. Barrett, M. Dryden, J. Cooke, D. Leaper and N. T. Georgopoulos, *Int. Wound J.*, 2017, **14**, 89–96.
35 P. Niethammer, C. Grabher, A. T. Look and T. J. Mitchison, *Nature*, 2009, **459**, 996–999.
36 R. Zhang, J. Zhao, G. Han, Z. Liu, C. Liu, C. Zhang, B. Liu, C. Jiang, R. Liu, T. Zhao, M. Y. Han and Z. Zhang, *J. Am. Chem. Soc.*, 2016, **138**, 3769–3778.
37 Z. Mao, H. Jiang, Z. Li, C. Zhong, W. Zhang and Z. Liu, *Chem. Sci.*, 2017, **8**, 4533–4538.
38 Y. Li, X. Xie, X. Yang, M. Li, X. Jiao, Y. Sun, X. Wang and B. Tang, *Chem. Sci.*, 2017, **8**, 4006–4011.
39 B. M. Lamb and C. F. Barbas III, *Chem. Commun.*, 2015, **51**, 3196–3199.
40 Z. Mao, L. Hu, X. Dong, C. Zhong, B.-F. Liu and Z. Liu, *Anal. Chem.*, 2014, **86**, 6548–6554.
41 C. G. Dai, J. L. Wang, Y. L. Fu, H. P. Zhou and Q. H. Song, *Anal. Chem.*, 2017, **89**, 10511–10519.
42 L. Zeng, S. Chen, T. Xia, W. Hu, C. Li and Z. Liu, *Anal. Chem.*, 2015, **87**, 3004–3010.
43 M. Petit, C. Tran, T. Roger, T. Gallavardin, H. Dhimane, F. Palma-Cerda, M. Blanchard-Desce, F. C. Acher, D. Ogden and P. I. Dalko, *Org. Lett.*, 2012, **14**, 6366–6369.
44 M. Pawlicki, H. A. Collins, R. G. Denning and H. L. Anderson, *Angew. Chem., Int. Ed.*, 2009, **48**, 3244–3266.
45 H. Kobayashi, M. Ogawa, R. Alford, P. L. Choyke and Y. Urano, *Chem. Rev.*, 2010, **110**, 2620–2640.
46 J. Chan, S. C. Dodani and C. J. Chang, *Nat. Chem.*, 2012, **4**, 973–984.
47 Y. L. Pak, S. J. Park, D. Wu, B. Cheon, H. M. Kim, J. Bouffard and J. Yoon, *Angew. Chem., Int. Ed.*, 2018, **57**, 1567–1571.
48 B. Wang, P. Li, F. Yu, P. Song, X. Sun, S. Yang, Z. Lou and K. Han, *Chem. Commun.*, 2013, **49**, 1014–1016.
49 H. Zhang, J. Liu, C. Liu, P. Yu, M. Sun, X. Yan, J. P. Guo and W. Guo, *Biomaterials*, 2017, **133**, 60–69.
50 C. Nathan and A. Cunningham-Bussel, *Nat. Rev. Immunol.*, 2013, **13**, 349–361.
51 D. André-Lévigne, A. Modarressi, M. S. Pepper and B. Pittet-Cuénod, *Int. J. Mol. Sci.*, 2017, **18**, 2149.